Progress In Electromagnetics Research M, Vol. 35, 31–38, 2014

Quasi Optical Effects of Non-Ionizing Radiation inside Pregnant Woman Abdomen

Md. F. Ali[1, *] and Sudhabindu Ray[2]

Abstract—Investigations have been carried out on the convex lens effect of non-ionizing radiation inside the abdomen of a pregnant woman. Focusing property for a plano-convex lens, which is thicker than twice of its focal length and filled with water, is studied for electric and magnetic fields at different microwave frequencies. It is observed that real image of electromagnetic fields are formed inside the lens itself at the focal plane when a microwave source is placed at a distance much greater than the twice the focal length. A three dimensional homogeneous electrical model of pregnant woman abdomen model behaves like plano-convex lens and creates real image of the microwave source inside the abdomen.

1. INTRODUCTION

Interaction of radiofrequency (RF) in the human body has been reported in several research articles [1–10]. In this paper, plano-convex lens like behaviour is investigated for a pregnant woman abdomen for non ionizing microwave radiation.

There have been increasing interests in the applications of numerical techniques to obtain the intensity of electric (E) and magnetic (H) fields in the human body models [11, 12]. Numerical electromagnetic (EM) methods play significant roles to calculate various Radio Frequency (RF) characteristics inside living objects including tissues or cells. Among all numerical methods, Finite Difference in Time Domain (FDTD) and Finite Integral Technique (FIT) are used in several research investigations during EM simulation of living tissues [13]. In the present work, FIT based commercially available software CST Microwave Studio® has been used to carry out the investigation to observe the lens effect of microwaves inside the abdomen of a pregnant woman at 925 MHz, 1.795 GHz and 2.1 GHz [14].

2. DIELECTRIC LENS

2.1. Microwave Thick Plano-Convex Lens

EM waves with microwave frequencies can be refracted, transmitted and reflected when it pass through a dielectric material object [15, 16]. Diffraction may occur from edges and corners of dielectric objects where the size of the object is similar to the wavelength. Thus, EM waves at microwave frequencies show many similarities like visible light [17].

Microwave lens is a dielectric structure which is transparent for microwave and capable of focusing or defocusing the EM energy of the microwave just like an optical lens focuses or defocuses visible light. Homogeneous dielectric materials of refractive index different from the free space have been used for a long time in microwave lens applications [18].

Received 7 January 2014, Accepted 11 February 2014, Scheduled 16 February 2014

* Corresponding author: Md. Faruk Ali (faruk_ali@rediffmail.com).

[1] Department of Electronics and Instrumentation Engineering, Nazrul Centenary Polytechnic, Rupnarayanpur, Burdwan, West Bengal 713335, India. [2] Department of Electronics and Telecommunication Engineering, Jadavpur University, Kolkata, West Bengal 700032, India.

A thick convex lens is shown in Fig. 1(a), where, S_1, S_2 are front and back vertices, and C_1, C_2 are front and back centre points, respectively. Focal length f of the lens is given by [19, 20]:

$$\frac{1}{f} = (n-1)\left[\frac{1}{R_1} - \frac{1}{R_2}\right] + \frac{t_c\,(n-1)^2}{nR_1R_2} \tag{1}$$

where, n is the refractive index of the lens medium, t_c thickness of the lens, and R_1 and R_2 are the radii of curvature of the lens. Placing a microwave source in front of such convex microwave lens at a distance more than focal length, an inverted real image of the source fields can be obtained [18, 21, 22]. Considering the quasi-optical microwave properties, image position may be obtained using the following rules [23].

Rule 1: Image is expected at f when object is located at infinity distance from lens,

Rule 2: Image is expected within f and $2f$ when object is located at more than $2f$ distance from lens and

Rule 3: Image is expected at $2f$ when object is located at $2f$ distance from lens.

If one of the surfaces of the convex lens is made flat, then it is transformed into a plano-convex lens. A thick plano-convex lens is shown in Fig. 1(b), where the f can be written as [20]:

$$f = \frac{R}{(n-1)} \tag{2}$$

where, n is the refractive index of the lens medium and R the radius of curvature of the plano-convex lens. Placing a microwave source in front of such plano-convex microwave lens at a distance more than focal length, an inverted image of the source can be obtained inside the lens when its thickness is more than the focal length.

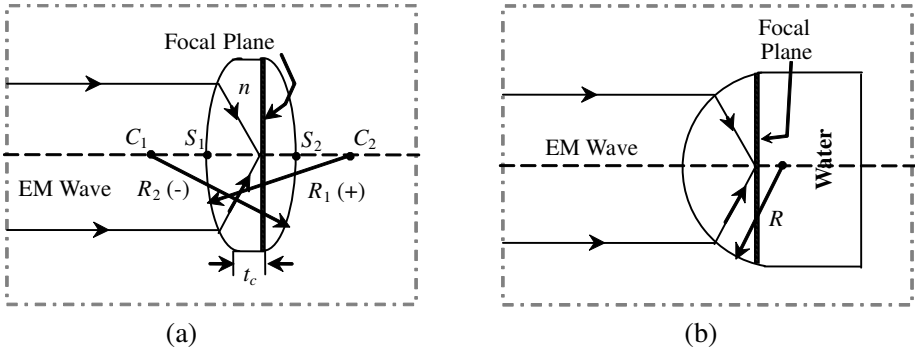

Figure 1. Geometry of thick (a) convex lens and (b) plano-convex lens.

3. STUDY ON THICK DIELECTRIC PLANO-CONVEX LENS

For simulation, a thick plano-convex lens filled with water along with a half-wave dipole antenna has been developed in CST Microwave Studio® as shown in the Fig. 2. The radius of curvature (R) of the plano-convex lens is 5.0 cm. A half-wave dipole antenna resonating at 2.0 GHz which acts as imaging object is placed at a distance (d) of 15.0 cm from the lens.

Value of the wavelength dependence refractive index (n) of water can be obtained from the relation: $n = \sqrt{\varepsilon_r}$, where, ε_r is relative dielectric constant of water [24]. From available literature the value of n is found to be $8.8043 + i0.4337$ at 2.0 GHz [25]. Thus, using Equation (2) focal length of this plano-convex lens is found to be 0.64 cm. The model is then simulated considering 465405 mesh cells. It is found that the E and H fields are focused at a distance of 0.64 cm, which is equal to the focal length of the lens itself. It is also observed that the image of source E and H fields is obtained inside the lens.

Distribution of E and H fields at the focal plane of the plano-convex dielectric lens as obtained from simulation is shown in Figs. 3(a) and (b), respectively. In Fig. 3(a), two high concentric spots consisting

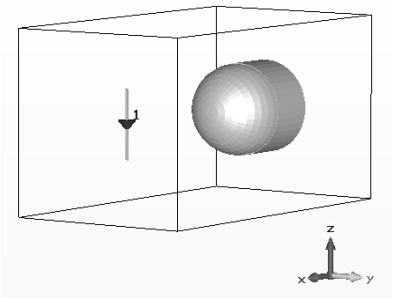

Figure 2. Geometry of the dielectric Plano-convex lens along with a half-wave dipole antenna.

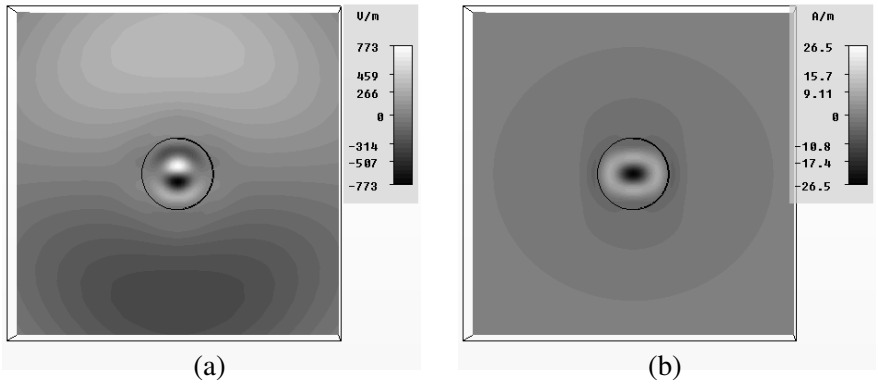

Figure 3. Distribution of (a) E field and (b) H field at the focal plane inside the lens.

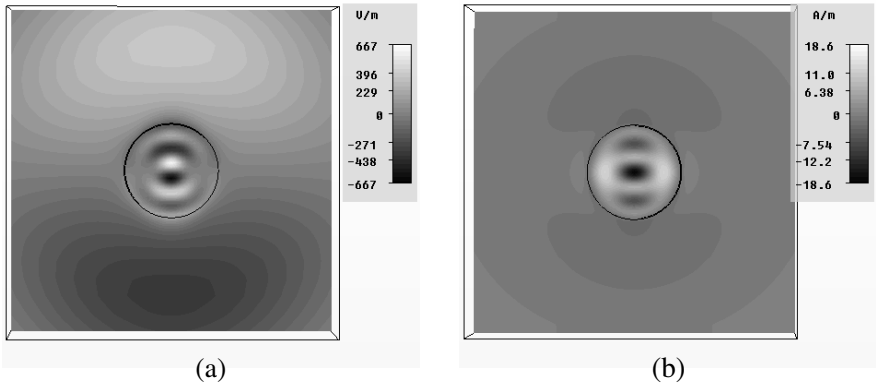

Figure 4. Phase value distribution of (a) E field and (b) H field at 0.5 cm from the focal plane inside the lens.

of different phases are observed at the focal plane. The phase difference between these two E fields is exactly 180°, as the phase difference of two poles of the source dipole. These two points represent the electrical field image of the source of the dipole antenna. For a dipole antenna, the maximum E field exists near the two ends of the dipole. Similarly, from Fig. 3(b), it can be observed that a single high concentric spot is formed at the focal plane. This point represents the high magnetic field formed at the source dipole antenna. For a resonating dipole antenna, the maximum H field exists at the centre of the dipole. In the focal plane, maximum E and H field intensity are 773 V/m and 26.5 A/m, respectively.

Distributions of E and H fields at 0.5 cm inner plane from the focal plane of the plano-convex dielectric lens are shown in Figs. 4(a)–(b). From Fig. 4(a), it can be observed that field distribution are

almost similar like earlier case, but maximum values of E and H field intensity at this plane are lower than that obtained at the focal plane due to the defocused fields. In this plane, maximum E and H field intensity are 667 V/m and 18.6 A/m, respectively.

Variation of absolute magnetic field $|H|$ with distance (D) measured from antenna end for $d = 15.0$ cm using different half-wave dipole antennas resonating at 925 MHz, 1795 MHz and 2.1 GHz respectively, is shown in Fig. 5. It is found that maximum magnetic field intensity inside the lens is obtained at the focal plane. Peak value of $|H|$ field intensity increases with the increase of frequency which is possibly due to the macroscopic diffraction from the dielectric edges. Diffraction effects are more intensive for dielectric size of similar to wavelength and line of site propagation is more intensive for larger dielectric size with compared to wavelength [26, 27].

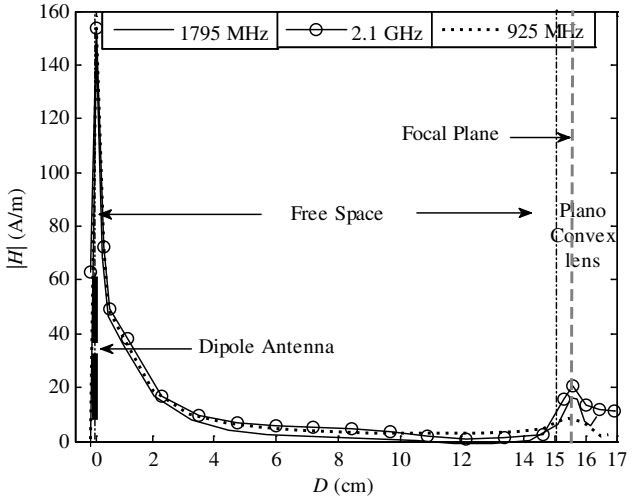

Figure 5. $|H|$ vs. D for $d = 15.0$ cm at 925 MHz, 1795 MHz and 2.1 GHz.

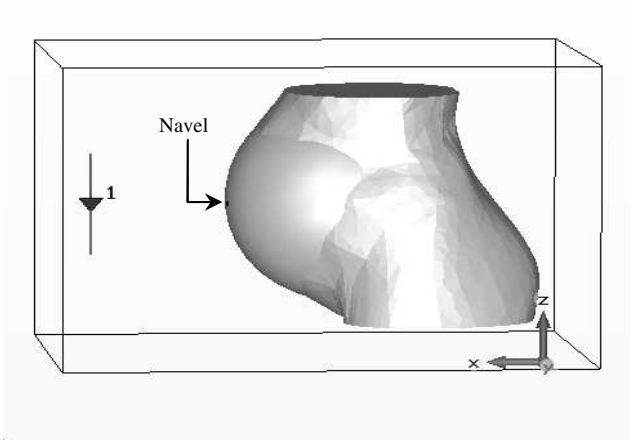

Figure 6. Simulation model of a pregnant woman abdomen model along with a dipole antenna.

4. STUDY ON LENS EFFECTS INSIDE A PREGNANT WOMAN ABDOMEN

The pregnant woman model has been constructed considering a 25 year old female with 65 kg weight and 5′4″ height [28]. To simplify the numerical model, other parts of the pregnant woman body except the full abdomen are excluded in the simulation. For further simplification, the pregnant body model is assumed to be comprised of only water. The abdomen of the pregnant woman model is comparable with a plano-convex lens with $R = 17.6$ cm and f of 2.3 cm.

Geometry of the pregnant abdomen along with a half-wave dipole antenna resonating at 925 MHz used in the simulation is shown in Fig. 6. Input power is of 20.0 W is considered for the simulation. The simulation performed consisting of 712356 mesh cells.

Variation of peak $|H|$ with depth, i.e., distance measured from the navel inside the pregnant woman model for a set of object distance (d) 10.0 cm, 20.0 cm, 30.0 cm, 40.0 cm and 50.0 cm at 925 MHz is shown in Fig. 7. It is found that a peak corresponding to the maximum value of $|H|$ is obtained at the plane where the fields are focused. For d more than or equal to 20.0 cm, H field is focused almost at the focal plane inside the pregnant woman abdomen and an image of magnetic field corresponds to the magnetic field at the centre of dipole is formed.

For $d = 10.0$ cm, image is obtained at the plane inside the pregnant woman model which is at the distance slightly more than the focal length. Unlike other curves, this curve shows large magnetic field at skin which is possibility due to increase of diffraction due to increase of angle of incident at various part of the convex area of abdomen.

Peak $|H|$ decreases with the increase of d and vice-versa. Variation of d (cm) with image distance (cm) obtained from the simulation at 925 MHz for the pregnant woman model is shown in the Table 1.

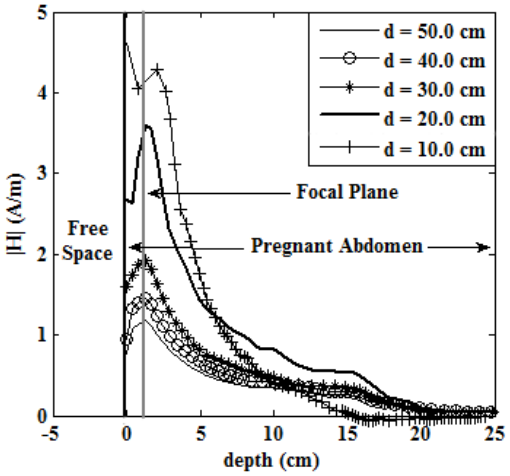

Figure 7. $|H|$ vs. depth for different object distances at 925 MHz.

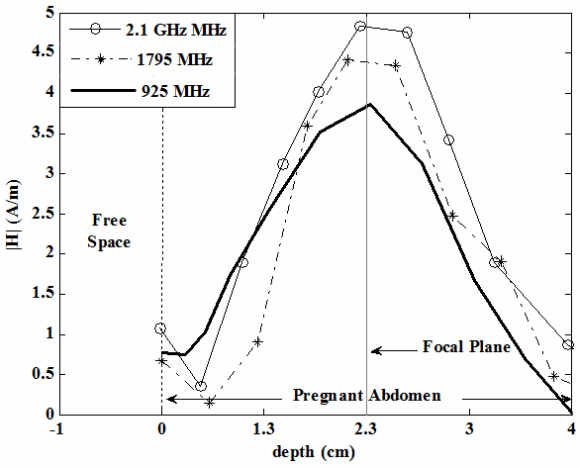

Figure 8. $|H|$ vs. depth for $d = 20.0$ cm at 925 MHz, 1795 MHz and 2.1 GHz.

Table 1. Variation of object distance with Image distance including peak $|H|$ for with and without woman model at 925 MHz.

Object distance (cm)	Image distance (cm)	Peak $\|H\|$ With woman model (A/m)	Peak $\|H\|$ Without woman model (A/m)
10.0	2.6	4.21	2.47
20.0	2.3	3.55	1.28
30.0	2.3	1.92	0.91
40.0	2.3	1.46	0.67
50.0	2.3	1.25	0.56

All the distances are measured from the navel of the pregnant woman abdomen. Therefore, it is seen that the pregnant woman model behaves like a plano-convex lens and follows classic principle of convex lens and for d more than or equal to 20 cm, quasi optical behaviour of microwave is prominent.

Maximum values of $|H|$ along the straight line passing through the mid-point of the dipole and navel point for different dipole antenna distances at 925 MHz are shown in the Table 1. It is found that for different antenna distances with woman abdomen model, peak value of $|H|$ is higher than that for the model without abdomen due to the focusing of fields from dielectric lens.

Variation of H with depth for $d = 20.0$ cm using different half-wave dipole antennas resonating at 925 MHz, 1795 MHz and 2.1 GHz respectively, is shown in Fig. 8. From the Fig. 8, it is found that peak $|H|$ is obtained at the focal plane inside the pregnant woman model and value of peak $|H|$ increases with the increase of frequency.

Field distributions using contour plots corresponding to H field obtained at the focal plane inside the pregnant woman abdomen for antenna distance of 20.0 cm at 925 MHz are shown in Figs. 9(a), (b). From Fig. 9(a), it can be observed that like the dielectric plano-convex lens, a single high concentric spot is formed at the focal plane because of the maximum H field exists close to the centre of the resonating dipole antenna. From contour line plots, it is found that the contour corresponding to the higher value of $|H|$ filed concentrates towards the focus.

A compact dual-band Planar Inverted Folded Antenna (PIFA) encapsulated mobile handset working at GSM bands with input power of 600 mW is placed 20.0 cm away form this pregnant woman abdomen model as shown in Fig. 10(c) [29, 30] to observe the electrical fields and specific absorption rate. The mobile handset configuration and its S-parameter (S_{11}) are shown in Figs. 10(a), (b). The PIFA of

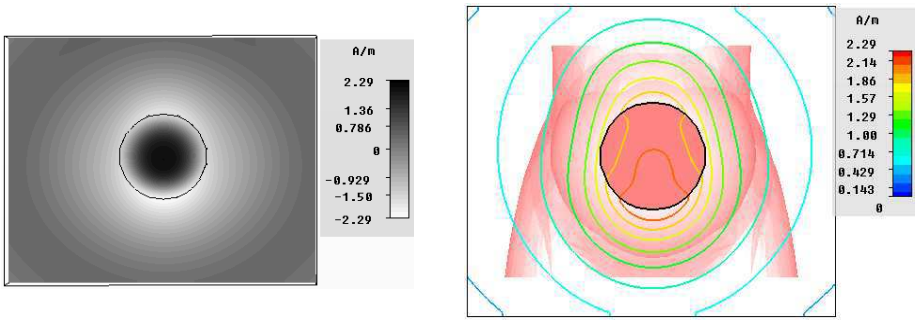

(a) (b)

Figure 9. (a) Phase and (b) contour line plots of H field at the focal plane inside the pregnant woman model at 925 MHz.

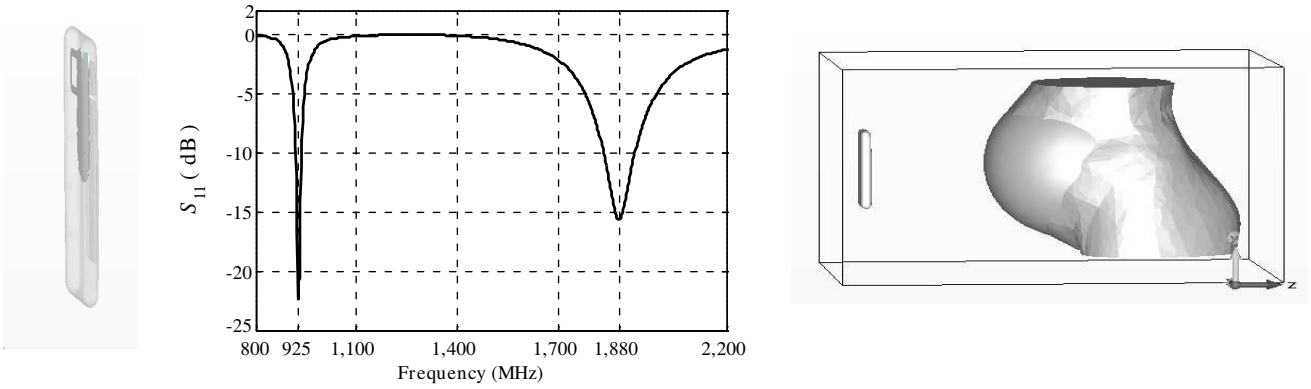

(a) (b) (c)

Figure 10. (a) Mobile handset, (b) S_{11} vs. frequency and (c) simulation model of pregnant woman model along with the mobile handset.

mobile handset resonates at 925 MHz with S_{11} of -22.41 dB and 1880 MHz with S_{11} of -15.68 dB at the fundamental and next higher mode, respectively. Peak value of $|E|$ and $|H|$ and Specific Absorption Rate averaged over 1-g of tissue (1-g SAR) induced inside the pregnant woman abdomen model are found to be 13.21 V/m, 0.028 A/m and 0.005 W/kg for 925 MHz at the focal plane. Although, the SAR value obtained is much lower than the IEEE/ICNIRP safety limits for non ionizing radiation [31], it may become critical for non-ionizing radiation from sources with higher radiation intensities.

5. CONCLUSION

In this paper, investigations have been carried out on the quasi optical behaviour of 925 MHz, 1.795 GHz and 2.1 GHz microwave and lens effects for a pregnant woman abdomen. Before carrying out the desired investigation, theory of microwave lens has been analysed developing water filled plano-convex dielectric lens having thickness more than double of its focal length. It is observed that real image of EM fields are formed inside the lens itself at the focal plane when a microwave source is placed at a distance much greater than twice of the focal length.

The E and H field strengths are investigated inside a three-dimensional electrical model of a pregnant woman abdomen for half-wave dipole antenna and compact dual-band PIFA encapsulated mobile handset working at GSM bands. Results obtained from the simulation show that the pregnant woman abdomen behaves as a plano-convex lens. It creates image of the microwave source and concentrates E and H fields at the focal plane. Image distance varies with the variation of the object distance, and it is found that when the object distance is much greater than the focal length, image is

formed at focus of the lens. Peak value of $|E|$, $|H|$ and 1-g SAR induced inside the pregnant woman abdomen near the focal plane for a mobile handset placed 20.0 cm away from the abdomen are found much below the IEEE/ICNIRP safety limits. However, sources placed at a distance more than twice of the focal length with similar frequency and high power may create high intensity field images at the focal plane. Similar effect is also expected at other body parts, such as abdomen of any other fatty person, breast, buttock, etc. Instead of single point, a linear path with concentrated fields is expected for the body parts with cylindrical structure. Particularly, for curved body parts, more EM fields may be concentrated near the focal region for microwave due to its quasi optical nature. In the whole study, isotropic dielectric with dielectric constant equal to water is considered. However, due to anisotropic nature behaviour, in actual case, the focussed fields may become blurred for regions with significant variation in dielectric constant.

REFERENCES

1. Islam, M. T., H. Z. Abidin, M. R. I. Faruque, and N. Misran, "Analysis of materials effects on radio frequency electromagnetic fields in human head," *Progress In Electromagnetics Research*, Vol. 128, 121–136, 2012.
2. Kesari, K. K., M. H. Siddiqui, R. Meena, H. N. Verma, and S. Kumar, "Cell phone radiation exposure on brain and associated biological systems," *Indian Journal of Experimental Biology*, Vol. 51, 187–200, March 2013.
3. Kumar, V., R. P. Vats, S. Goyal, S. Kumar, and P. P. Pathak, "Interaction of electromagnetic radiation with human body," *Indian Journal of Radio & Space Physics*, Vol. 37, 131–134, April 2008.
4. Ali, M. F. and S. Ray, "SAR analysis in a spherical inhomogeneous human head model exposed to radiating dipole antenna for 500 MHz–3 GHz using FDTD method," *International Journal of Microwave and Optical Technology*, Vol. 4. No. 1, 35–40, 2009.
5. Lin, J. C., "Malignant brain tumors from cellular mobile telephone radiation," *IEEE Antenna and Propagation Magazine*, Vol. 49, No. 1, 212–214, February 2007.
6. Virtanen, H., J. Keshvari, and R. Lappalainen, "Interaction of radio frequency electromagnetic fields and passive metallic implants — A brief review," *Bioelectromagnetics*, Vol. 27, No. 6, 431–439, September 2006.
7. Salford, L., "Experimental studies of brain tumor development during exposure to continuous and pulsed 915 MHz radio frequency radiation," *Bioelectrochemistry and Bioenergetics*, Vol. 30, 313–318, 1993.
8. Lak, A., "Human health effects from radiofrequency and microwave fields," *Journal of Basic and Applied Scientific Research*, Vol. 2, No. 12, 12302–12305, 2012.
9. Jiao, C. and L. Gao, "Progress in studies of radio frequency radiation of the wireless communication device," *PIERS Proceedings*, 945–949, Xian, China, Mar. 22–26, 2010.
10. Karpowicz, J. and K. Gryz, "An assessment of hazards caused by electromagnetic interaction on humans present near short-wave physiotherapeutic devices of various types including hazards for users of electronic active implantable medical devices (AIMD)," *BioMed. Research International*, Hindawi, Vol. 2013, Article ID 150143, August 2013.
11. Sanchez, C. C., P. Glover, H. Power, and R. Bowtell, "Calculation of the electric field resulting from human body rotation in a magnetic field," *Physics in Medicine and Biology*, Vol. 57, 4739–4753, 2012.
12. Psenakova, Z., "Numerical modeling of electromagnetic field effects on the human body," *Advances in Electrical and Electronic Engineering* Vol. 5, Nos. 1–2, 319–322, ISSN 1336-1376.
13. Samaras, T., P. Regli, and N. Kuster, "Electromagnetic and heat transfer computations for non-ionizing radiation dosimetry," *Physics in Medicine and Biology*, Vol. 45, No. 8, 2233–2246, 2000.
14. CST Microwave Studio Suite 2010, available at: http://www.cst.com.
15. Preston, D. W. and E. R. Dietz, *The Art of Experimental Physics*, Wiley, New York, 1991.

16. Murray, W. H., "Microwave diffraction techniques from macroscopic crystal models," *American Journal of Physics*, Vol. 42, 137, July 1974.
17. Kezerashvili, R. Y., "Light and electromagnetic waves teaching in engineering education," *International Journal of Electrical Engineering Education*, Vol. 46, No. 4, 343–353, November 2007.
18. Cornbleet, S., *Microwave Optics*, Academic Press, New York, 1976.
19. Greivenkamp, J. E., *Field Guide to Geometrical Optics*, SPIE Press, 6–9, 2004, ISBN 978-0-8194-5294-8.
20. "Laser components Gmbh: Lens theory, singlet lenses," Available: www.lasercomponents.com.
21. Levanda, R. and A. Leshem, "Image formation in synthetic aperture radio telescopes," 1–13, September 2, 2010, Available: http://arxiv.org/pdf/1009.0460.pdf.
22. Shi, Z., Y. Nagayama, D. Kuwahara, T. Yoshinaga, M. Sugito, and S. Yamaguchi, "Two-dimensional numerical simulation of microwave imaging reflectometry," Vol. 8, *J. Plasma Fusion Res. Series*, 2009.
23. Dou, W. B., H. F. Meng, B. Nie, Z. X. Wang, and F. Yang, "Scanning antenna at THz band based on quasi-optical techniques," *Progress In Electromagnetics Research*, Vol. 108, 343–359, 2010.
24. From Wikipedia: Refractive index, Available: http://www.videosec.com/education/Refractive-index.pdf.
25. Segelstein, D., "The complex refractive index of water," M.S. Thesis, University of Missouri-Kansas City, 1981.
26. Kapany, N. S., J. J. Burke, Jr., and K. Frame, "Diffraction by apertures of wavelength dimensions," *Applied Optics*, Vol. 4, No. 10, 1229–1238, 1965.
27. Sarkar, T. K., Z. Ji, K. Kim, A. Medour, and M. Salazar-Palma, "A survey of various propagation models for mobile communication," *IEEE Antennas Propag. Mag.,* Vol. 45, No. 3, 51–82, 2003.
28. Make Human^{TM}, Available: http://www.makehuman.org.
29. Yeh, S. H., K. L. Wong, T. W. Chiou, and S. T. Fang, "Dual-band planer inverted F antenna for GSM/DCS mobile phones," *IEEE Trans. on Antennas and Propagation*, Vol. 51, 1124–1126, 2003.
30. Islam, M. T. and M. R. I. Faruque, "Reduction of specific absorption rate (SAR) in the human head with ferrite material and metamaterial," *Progress In Electromagnetic Research C*, Vol. 9, 47–58, 2009.
31. ICNIRP Guidelines, "Guidelines for limiting exposure to time-varying electric, magnetic and electromagnetic fields upto 300 GHz," *Health Physics*, Vol. 74, No. 4, 508–509, 1982.